Transmission Characteristics of Finite-Width Conductor-Backed Coplanar Waveguide

Ching-Cheng Tien, Ching-Kuang C. Tzuang, *Senior Member, IEEE,* S. T. Peng, *Fellow, IEEE,* and Chung-Chi Chang

Abstract— This paper presents theoretical and experimental results for a finite-width conductor-backed coplanar waveguide (FW-CBCPW). The guiding characteristics of FW-CBCPW are investigated first by the rigorous method of mode matching. An FW-CBCPW through line is then placed within a test fixture commonly used in laboratories, and the scattering parameters of the through line are obtained theoretically by approximating the FW-CBCPW as a simple system of coupled transmission lines. Experimental results are shown to agree very well with the theoretical ones. In particular, the anomalous behavior observed in the transmission characteristic of the through line is related to the resonant phenomenon of the terminated side planes which are short-circuited at both input and output ends due to the test fixture. Finally, a technique of mode suppression in the side-plane regions is suggested for the improvement of signal transmission over a broad band of frequency spectrum. The effects of extra higher order modes on the transmission characteristics at high frequencies are also discussed.

I. INTRODUCTION

A COPLANAR WAVEGUIDE (CPW) may be viewed as a structure composed of two symmetrically coupled slot lines [1]. The most important feature of this type of structure is that the signal line and ground planes are all placed on one side, say the upper side, of the substrate. Thus, a circuit consisting of passive components and active devices can be implemented by CPWs with relative ease [2]–[5]. In contrast, the widely used microstrip line has its ground plane placed on the back side of the substrate; consequently, a circuit element has to be connected through via holes if grounding is required. In practice, however, a coplanar monolithic microwave and millimeter-wave integrated circuit (CMMIC) is usually placed on a ground plane for mechanical support, Because the GaAs substrate is typically thin and fragile; this gives rise to the conductor-backed CPW (CBCPW) [6]. Furthermore, the substrate and upper ground planes (side planes) are always of finite width; as a result, we generally have finite-width conductor-backed coplanar waveguide (FW-CBCPW) which may be viewed alternatively as a system of three coupled microstrip lines, instead of two coupled slot lines. With such an alternative viewpoint, many network characteristics of FW-CBCPW can be easily analyzed and explained. Finally, when an FW-CBCPW of certain length,

namely, a through line, is put within a test fixture, the effect of the measuring apparatus has to be taken into account. A theoretical study of FW-CBCPW in such a laboratory setting still remains to be explored.

In this paper, we shall take the alternative viewpoint of coupled microstrip lines for the analysis of an FW-CBCPW through line. Specifically, the structure under investigation is explained in Section II, together with a summary of the literature on the subject. In Section III, an exact method matching is employed, first to determine the guiding characteristics of FW-CBCPW, and the results are then utilized for an approximate analysis of a symmetric FW-CBCPW through line in terms of a four-port network consisting of two coupled transmission lines [7]–[9]. The width of side planes, however, is limited to such an extent that its first higher order leaky mode is below cut-off [10] in the frequency range of interest from almost dc to 26.5 GHz. Section IV compares the theoretical results with the measured ones. The anomalous behavior associated with the transmission coefficient of the through line is related to the resonances of the side-plane regions which are short-circuited at both input and output ends. Furthermore, in Section V, it is shown that by shorting the lateral edges of the two side planes, the unwanted zero-cut-off propagating mode will no longer exist and the resonances of the side-plane region are then suppressed. Experimental results are given to confirm that the transmission can indeed be improved over a wide band of frequency. Such approach of mode suppression should be made with caution, because another type of extra higher order mode will appear above certain threshold frequency, upon which the anomalous resonant phenomenon will start to appear. Finally, some conclusions are given in Section VI.

II. STATEMENT OF PROBLEM AND BRIEF SUMMARY OF LITERATURE

Fig. 1 shows the cross-sectional geometry of an FW-CBCPW under investigation, with the coordinate system also attached. It consists of three coplanar metal strips of finite width, W and W_G for the center and side strips, respectively. The metal strips have a small thickness t and a large but finite conductivity σ, and the distance between two neighboring strips is denoted by S. The substrate has dielectric constant ϵ_r, a thickness h, and a finite width with an excessive portion denoted by W_D on each side. The structure is placed on a thick ground plane for mechanical support. In order to discretize the modes in the vertical direction, a perfectly
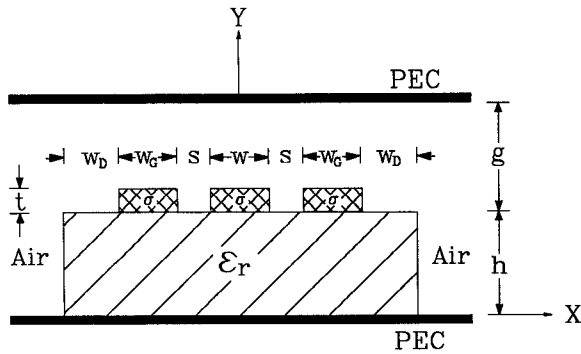
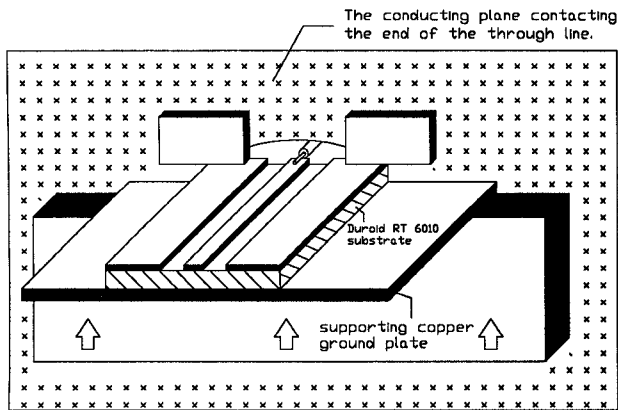Fig. 1.   Cross-sectional geometry of an FW-CBCPW.

Fig. 2.   An artistic view of CASCADE MTF-26 microstrip/CPW test fixture mounted with an FW-CBCPW through line. Only one test port is shown. The conducting plane at input or output is shaded with the cross symbols.

conducting plate is placed at a distance above the structure. Since the guided energy is mostly confined under the metal strips, the introduction of the extra conducting plate at a sufficiently large distance will not perturb significantly the guiding characteristics of the structure. We had presented an exact formulation of such a general structure by the method of mode matching [11]–[14], and the results previously obtained will be utilized here.

Fig. 2 depicts one example of testing a CPW through line circuit. Each of input port and output port of the CPW test fixture has a conducting plane allowing a small hole for probe contact. The test condition shown in Fig. 2 is different from that of the on-wafer CPW probe system [15], [16], where the CPW probes make contact on the CPW circuit and there are no conducting planes near the probe tips. Fig. 2 also reflects a much more realistic test condition if one considers that the CMMIC has been separated and placed into a metallic housing or similar environments allowing external connections for signal ports. Shih also reported a similar arrangement to Fig. 2 for the on-wafer testing of the CBCPW through line or the shorted line [17]; he applied via holes at both ends of side planes near the center signal line. The main purpose of this paper is to study the transmission characteristics of FW-CBCPW through line within a test fixture, as shown in Fig. 2.

In what follows, a brief account of researches conducted on the CPW is summarized. The characterization and development of CPW technology have gradually evolved since its introduction in 1969 [1]. C. P. Wen formulated a quasi-static conformal mapping method to obtain the propagation constant and the characteristic impedance of the dominant CPW mode. Knorr [18] adopted the spectral-domain approach (SDA) [19] and reported the dispersive propagation characteristics of the CPW. Kitazawa [20] and Sorrentino et al. [21] reported the effects of metal thickness on the CPW by using the full-wave approach. The slow-wave propagation of the CPW has been extensively investigated by Itoh and his co-workers [22]–[25].

Although the back-side ground plane is not required for supporting the CPW mode, the CPW is subject to the influence of the lower ground plane in practice. Itoh and Shih first investigated the dominant CPW mode propagation of the so-called conductor-backed CPW (CBCPW) using the full-wave SDA [6]. It has been found that the influence of the ground plane on the propagation characteristics can be significant when the substrate thickness becomes comparable to the slot width.

In the CBCPW with a semiconductor substrate mounted on low-permittivity buffer layer, the short circuit and discontinuity may cause parasitic radiation effects due to the generation of parasitic modes such as space waves and surface waves [26]–[27]. The most likely excited parasitic modes in these circuits are the parallel-plate transmission-line modes. Besides the parasitic radiation effect, the conductor backing may result in the leakage of power into the dielectric-filled parallel-plate regions at all frequencies [28]. The leakages associated with the conductor-backed slot line and the coplanar waveguide (CPW) also depend on the lateral extent (width) of either the conductor backing or the side planes constituting the slot line or the CPW. In some cases, as shown in [28]–[30], the surface-wave leakages occur at higher frequencies for CPW or slot lines with finite-width side planes (See [28, p. 201, Fig. 1]). The effect of finite-width side planes of CPW or CBCPW on transmission characteristics can not be neglected.

The microstrip-like mode (MSL) can result from the CPW of finite-width side planes with or without the conductor backing. Jackson identifies this as a coplanar microstrip mode (CPM) for CPW with conductor backing [31], while Shigesawa and Tsuji name this as a CPW surface-wave-like (SWL) mode. The aforementioned parasitic TM_0 parallel-plate mode or surface wave excited by the discontinuities now may be converted into the bounded MSL mode. Thus the CPW structure is overmoded. When the substrate is of finite extent, the conventional CPW mode and the MSL mode constitute two dominant modes below a critical frequency. Above the critical frequency, a leaky wave in the form of TM_o surface wave or TE_o surface wave will occur for the case with or without conductor backing, respectively. In the overmoded CPW circuits, the mode conversion among the incident, transmitted and reflected waves will take place. The CBCPW-MS discontinuity problem of various gap ends has demonstrated such mode conversion process [31]. When an additional substrate of lower dielectric constant is attached right below the GaAs substrate, the CPW mode and microstrip-

like mode may become matched in phase and strong mode coupling may occur at certain frequency. The conversion gain, i.e., the percentage of incident CPW mode converted to the MS mode, shows a resonance-like response at 60 GHz for certain thickness of the additional substrate [31]. When mode conversion of mode coupling appear in the CPW circuit, the electromagnetic energy is no longer confined in the vicinities of CPW slot surfaces; rather, the energy may be carried away by the microstrip-like mode, leaky wave, or other higher order modes, depending on the frequency of operation and the waveguiding structure. Such non-CPW type of energy can couple itself to the neighboring circuits and produce a crosstalk in the CPW circuit. One example is given in [32] showing the dynamic coupling of a narrow-pulse transmission on conventional CPW into its nearby short-circuited CPW.

Considerable efforts have been devoted to the reduction of interferences in the overmoded CBCPW circuits. For examples, the increase of substrate thickness and side-plane width can decrease the excitation energy of MSL mode [33], and the additional buffer layer can decrease the conversion gain of MSL mode in the gap end of FW-CBCPW circuit [31] and eliminate the leakage problems in CBCPW MICs [34].

Because of the symmetry of the structure, a magnetic wall may be placed in the middle of the signal line for the symmetric modes. Fig. 3 illustrates the cross-sectional electric field lines of the symmetric modes in an FW-CBCPW of finite-width substrate and side planes. The dominant CPW mode has its field pattern sketched in Fig. 3(a). The energy may leak away from the dominant CPW mode if the substrate were extended to infinity; however, it is now totally reflected by the lateral dielectric boundaries and it becomes bounded in the case of finite-width substrate [14]. The MSL mode, as shown in Fig. 3(b), is another propagating mode resembling the parallel-plate transmission-line mode. Note that such MSL mode inherently exists in the FW-CBCPW circuit if no other means of mode suppression are applied. If the side planes are wider, the next higher order MSL mode may exist, as shown in Fig. 3(c). There exists one change over the electric field pattern underneath the side plane. Fig. 3(d) sketches the image-guide-like propagating model provided the substrate is protruded further away from the side plane. The leaky waves will occur for those higher order modes other than the CPW mode (Fig. 3(a)), the MSL mode (Fig. 3(b)), and image-guide-like mode (Fig. 3(d)), which exhibit the propagation characteristics of zero cut-off frequency. On the other hand, the higher order MSL mode shown in Fig. 3(c) can leak below certain onset frequency since its phase constant is less than free space wavenumber k_o.

The aforementioned overmoded CBCPW circuit of finite-width side planes and finite-width substrate should be investigated on its propagation characteristics thoroughly. Given an overmoded FW-CBCPW through line placed in a test fixture with vertical conducting side walls attached to both input and output ports of the through line, this paper aims to investigate theoretically and experimentally its transmission characteristics and explains physically how the observed resonances are related to the overmoded situation.
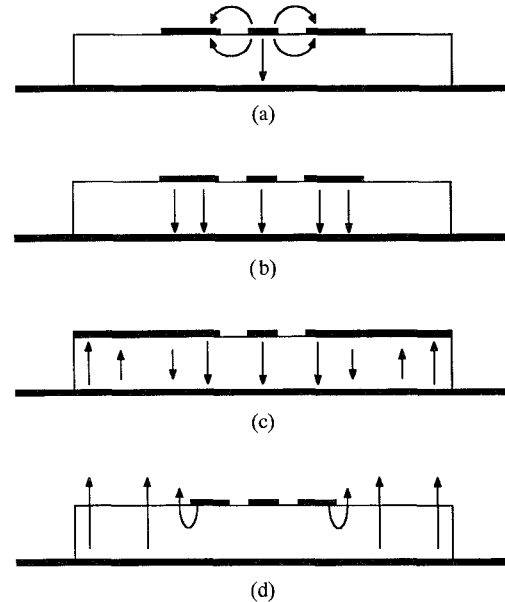

Fig. 3. The symmetric modes of an overmoded CBCPW of finite-width side planes and finite-width substrate. (a) CPW mode. (b) MSL mode. (c) First higher order MSL mode. (d) Image-guide-like mode.

III. ANALYSIS: THE APPROXIMATE 2N-PORT NETWORK APPROACH

A. The dispersion Characterisitcs (Mode Spectrum) of the FW-CBCPW

The structure of interest shown in Fig. 1 had been formulated exactly [14], and a computer program for the computation of dispersion roots has been implemented and will be used in this work. It is noted that the network representation of full-wave mode-matching method incorporating the metal modes [11]–[14] was invoked to obtain the propagation characteristics including the complex parameters such as the Poynting powers, currents on the coplanar strips and complex propagation constants. In out particular case study, the structural parameters and the material constants are so chosen that the structure supports only the CPW mode and the MSL mode below 26.5 GHz. Fig. 4 shows the dispersion characteristics of an FW-CBCPW together with its structural parameters and material constants. The dimensions of the FW-CBCPW are also compatible to the MTF-26 fixture. The resulting FW-CBCPW has its CPW mode exhibiting 50 Ω characteristic impedance when $W_G = \infty$.

Note that the next higher order mode shown in Fig. 3(c) leaks below certain onset frequency, which is 36.8 GHz for the same structure mentioned above. Below 26.5 GHz, the normalized phase constant of leaky wave β/k_o approaches to zero and the normalized attenuation constant α/k_o grows rapidly and exceeds unity. The leaky mode then goes below cut-off as discussed in [10] and is assured to exert a negligible effect on the leaky-wave loss in our measured frequency range. The other higher order modes also have negligible contribution to leakage loss. Although the top cover is considered in our analysis, the similar leaky-wave phenomena are also presented
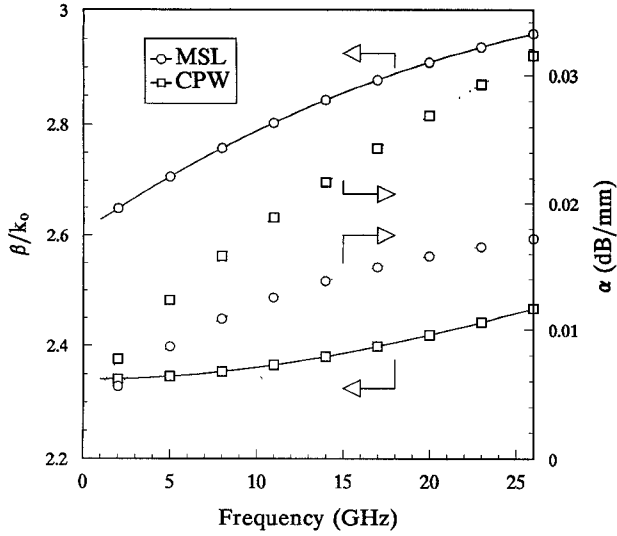
Fig. 4. Dispersion characteristics of the FW-CBCPW as shown in Fig. 1. -o- Normalized phase constants of MSL mode; ..o.. Attenuation constants of MSL mode; -□- Normalized phase constants of CPW mode; ..□.. Attenuation constants of CPW mode. The structural parameters are listed as follows: $W = S = 0.508$ mm, $W_G = 1.0$ mm, $W_D = 0.0$ mm, $h = 0.2$ $g = 0.635$ mm, $t = 17\mu$m, $\sigma = 5.8 \times 10^7$ S/m (copper), and $\epsilon_r = 10.2$.

with the top cover removed and the leakage loss can still be neglected in our particular case study.

As frequency decreases, the MSL mode no longer confines its electromagnetic energy underneath the metal strips but more energy spreads into the nearby air region. Because of this proximity effect in the presence of the finite-width substrate [35], the normalized phase constants of the MSL mode, as denoted by solid line and circular symbols in Fig. 4, greatly decrease in the low frequency limit.

B. The Equivalent 4-Port Model and Its Normalizing Impedances

Under the physical conditions described in the preceding section, we may use a very effective method of approximation to obtain the S-parameters of an FW-CBCPW through line provided only the CPW mode and MSL mode are excited. In this way, the coupling between the signal line and the finite-width side planes and the response of the overmoded FW-CBCPW through line to the test condition of Fig. 2 thoroughly depend on the excitation of CPW mode (Fig. 3(a)) and MSL mode (Fig. 3(b)). We incorporate a 2N-port model of $(N+1)$ coupled transmission lines. The N dominant modes are applied to investigate the overmoded FW-CBCPW through line. Because of the symmetry, a magnetic wall is placed at the center of the signal strip; only half of the equivalent circuit needs to be shown. The width of the side planes, however, is limited to a certain extent that the next higher order mode such as the one shown in Fig. 3(c) is well below cut-off [10] at the highest frequency limit of our study, i.e., 26.5 GHz. Only the two possible modes will contribute to the transmission characteristics of the through line. These two modes are always present since the CBCPW has finite ungrounded side planes. The FW-CBCPW through line now becomes a 4-port microwave network, i.e., N is equal to 2
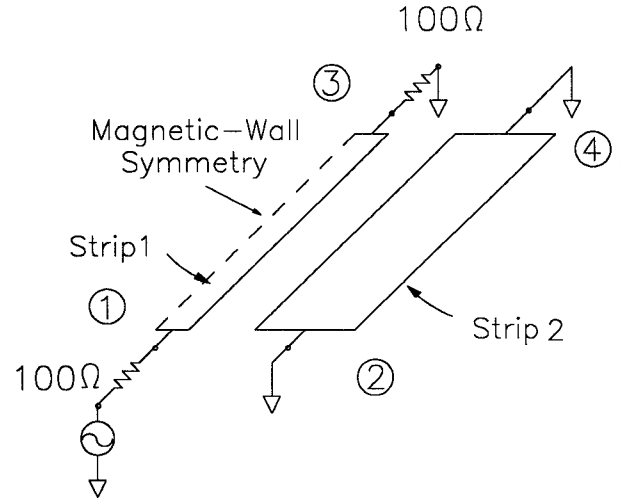

Fig. 5. A 4-port circuit model for a symmetric FW-CBCPW through line shown in Fig. 1 with its normalizing impedances reflecting the terminating condition of Fig. 2.

in our analysis. Fig. 5 shows the equivalent circuit of Fig. 2 for a coplanar-strip through line. Referring to Fig. 2, where an FW-CBCPW through line is mounted on the MTF-26 test fixture, two ends of center signal line are connected with the 50 Ω probe tips. The two side planes of the FW-CBCPW contact the conducting side wall of the fixture. Therefore, the ports 2 and 4 of Fig. 5 are connected to ground. Because of the half circuit, the normalizing impedances for ports 1 and 3 are doubled to 100 Ω. Thus the terminating conditions for the 4-port system are defined and its corresponding normalizing impedance matrix is shown as

$$[Z_o] = \begin{bmatrix} 100 & 0 & 0 & 0 \\ 0 & 0 & 0 & 0 \\ 0 & 0 & 100 & 0 \\ 0 & 0 & 0 & 0 \end{bmatrix} \quad (1)$$

C. The Scattering Parameters of the FW-CBCPW Through Line

When the Poynting powers P_{CPW} and P_{MSL} are obtained for CPW mode and MSL mode, respectively in Fig. 4, we may define the power matrix $[P]$ and the eigen-current matrix $[M_I]$ as follows [8], [11], [12]:

$$[P] = \begin{bmatrix} P_{\text{CPW}} & 0 \\ 0 & P_{\text{MSL}} \end{bmatrix} \quad (2)$$

and

$$[M_I] = \begin{bmatrix} I_{1\text{CPW}} & I_{1\text{MSL}} \\ I_{2\text{CPW}} & I_{2\text{MSL}} \end{bmatrix} \quad (3)$$

where subscripts 1 and 2 denote strip 1 and strip 2 of Fig. 5. For example, $I_{2\text{CPW}}$ is the CPW-mode current flowing in strip 2 of Fig. 5. After obtaining the complex propagation constants, γ_{CPW} and γ_{MSL}, the matrix $[P]$ and $[M_I]$, the well-known 2N-port admittance matrix [8] is given by

$$[Y_{2N}] = \begin{bmatrix} [Y_a] & [Y_b] \\ [Y_b] & [Y_a] \end{bmatrix} \quad (4)$$

where

$$[Y_a] = [M_I][\coth(j\gamma_i l)]_{\text{diag}}[P]^{-1}[M_I]^* \quad (5)$$
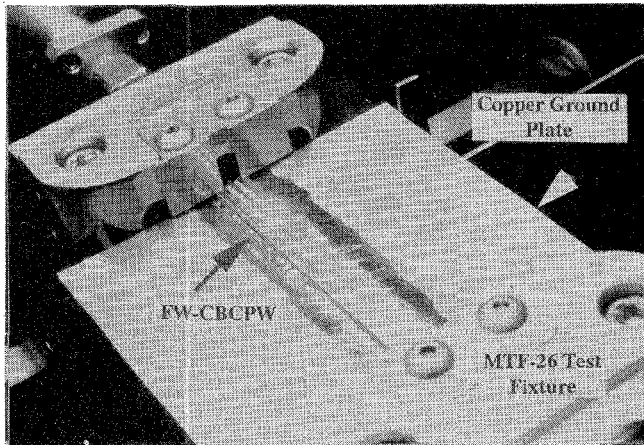
Fig. 6. The photograph of the FW-CBCPW through line mounted on the CASCADE MTF-26 test fixture.

and

$$[Y_b] = [M_I][-\text{csch}(j\gamma_i l)]_{\text{diag}}[P]^{-1}[M_I]^* \qquad (6)$$

where l is the physical length of the through line. The asterisk (*) denotes the conjugate transpose of the matrix manipulation. Invoking (1) and (4), we can obtain the $[S]_{4\times4}$ matrix describing the FW-CBCPW through line under proper termination [36]

$$[S]_{4\times4} = [Z_o]^{1/2}([Z_o]^{-1}-[Y_{2N}])([Z_o]^{-1}+[Y_{2N}])^{-1}[Z_o]^{-1/2}. \qquad (7)$$

The 2-port S-matrix $[S]_{2\times2}$ of the FW-CBCPW through line then can be extracted from the 4-port scattering matrix $[S]_{4\times4}$, i.e.,
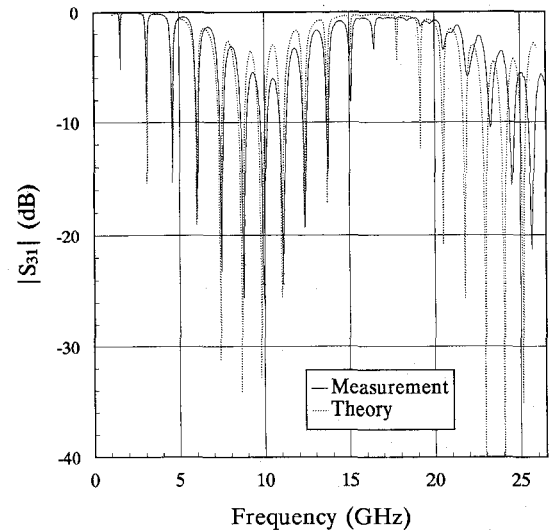
$$[S]_{2\times2} = \begin{bmatrix} S_{11} & S_{13} \\ S_{31} & S_{33} \end{bmatrix} \qquad (8)$$

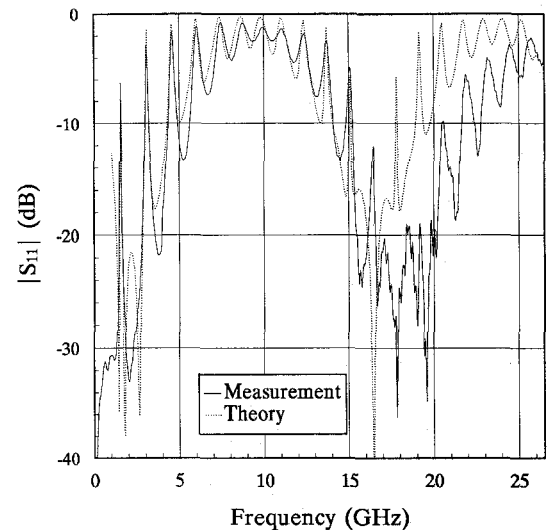in which we must have $S_{13} = S_{31}$, since the through line is reciprocal.

IV. THEORETICAL RESULTS AND EXPERIMENTAL VERIFICATION

Fig. 6 is the photograph of the FW-CBCPW through line test setup using the CASCADE MTF-26 test fixture. The FW-CBCPW through line under test consists of an RT/duroid™ 6010 substrate and a wide copper ground plate. The through line length L is equal to 38.1 mm. The measured S-parameters of the FW-CBCPW through line are obtained by the HP8510 network analyzer swept from 0.066 GHz to 26.5 GHz.

Figs. 7(a) and (b) compare the theoretic and experimental data for the magnitude of transmission coefficient ($|S_{31}|$) and reflection coefficient ($|S_{11}|$) of the FW-CBCPW through line, respectively. Both plots show that the theoretic results are in very good agreement with the measured values. Many resonant points are observed in Fig. 7. They are separated by approximately equal frequency interval. In other words, these resonant frequencies show certain periodicity. When the FW-CBCPW through lines resonates, only small amounts of electromagnetic energy can be transferred and most energy is

Fig. 7. Comparison of the theoretic and measured results of the FW-CBCPW through line as shown in Fig. 1. The through line length is equal to 38.1 mm. (a) $|S_{31}|$. (b) $|S_{11}|$.

reflected at input end. This can be clearly seen by overlaying Figs. 7(a) and (b). Such phenomenon severely deteriorates the CBCPW circuit performance. In CMMIC such phenomenon will also jeopardize the desired circuit response.

In view of Figs. 2, 5, and 6, the resonance should occur between the two vertical conducting walls of the test fixture since the other two sides are unbounded. In other words, it looks like a transmission-line resonator with its electromagnetic energy reflected between the two conducting side walls. Furthermore, the CPW mode has its electromagnetic energy confined near the slot surfaces and it can propagate through the tiny hole of the fixture and reaches to the external coaxial cable. In contrast, the MSL mode has its electric field lines polarized vertically underneath the metal strips (See Fig. 3(b)) and parallel to the two conducting side walls of the test fixture. Consequently, the MSL mode can hardly propagate through the tiny hole and is reflected back and forth inside the test

TABLE I
LIST OF THE RESONANT FREQUENCIES OBTAINED FROM MEASUREMENT, THEORETICAL RESULTS, AND
THOSE SOLVED FROM (9) FOR MSL MODE AND (10) FOR CPW MODE.

nth Resonance	Measurement	4-Port Model (Theory)	Equation (9) (MSL mode)	Equation (10) (CPW mode)
1	1.55	1.55	1.49	1.68
2	3.07	3.10	2.95	3.36
3	4.63	4.60	4.38	5.03
4	6.05	6.00	5.79	6.70
5	7.47	7.40	7.17	8.36
6	8.79	8.65	8.54	10.0
7	9.95	9.80	9.89	11.6
8	11.1	11.0	11.2	13.3
9	12.4	12.4	12.5	14.9
10	13.7	13.7	13.8	16.4
11	15.0	15.0	15.2	18.0
12	16.4	*	16.5	19.6
13	*	17.8	17.7	21.1
14	19.2	19.2	19.0	22.6
15	20.5	20.5	20.3	24.1
16	21.9	21.8	21.6	25.6
17	23.3	23.0	22.8	
18	24.5	24.1	24.1	
19	25.7	25.2	25.3	

Unit: GHz

fixture; therefore, the observed resonances should be attributed to the excitation of the MSL mode.

Table I extracts the resonant frequencies shown in Figs. 7(a) and (b). They appear in the second and third columns of Table I for the measured and theoretic data, respectively. The resonant frequencies obtained from both measurement and theory agree up to the seventeenth resonance. The last two resonant frequencies, the 18th and the 19th, deviate slightly by approximately 0.5 GHz.

The fourth column invokes the following equation for determining the resonant frequencies if the MSL mode is assumed to contribute to the half-wavelength transmission-line resonator.

$$\beta_{\text{MSL}}(f_n) \times L = n\pi. \tag{9}$$

Table I clearly shows that the resonant frequencies obtained by (9) agree very well with both measured and theoretic data. It is apparent that the anomalous phenomenon is due to the excitation of the MSL mode inherently existing in the FW-CBCPW through line. For the purpose of comparative study, if we assume that the CPW mode provides the resonance and applies the similar equation, i.e.,

$$\beta_{\text{CPW}}(f_n) \times L = n\pi \tag{10}$$

the results are listed in the fifth column of Table I. The resonant frequencies thus obtained are very different from both measured and theoretic data. Apparently, the resonant phenomenon is not caused by the CPW mode.

As long as the FW-CBCPW through line can be treated as the coupled transmission-line system, it becomes overmoded. The input signal appearing in the center strip will be coupled to the two top side planes, where the signals are reflected by the short-circuited terminations at input and output ends of the finite-width side planes. Considering a general CBCPW circuit, if two adjacent FW-CBCPW transmission lines have

a common top side plane, based on the results shown in Figs. 7(a) and (b) and Table I, it will not be difficult to imagine that the coupling and crosstalk between signal lines are inevitable. Furthermore, once the resonance occurs in the CBCPW circuit, severe degradation in circuit performance can be observed.

The asterisks shown in Table I indicate that no sharp resonance exists and a very good transmission of power is obtained. At the 12th resonant frequency, i.e., 16.5 GHz, the phase difference between the CPW mode and the MSL mode at the output port is almost 2π. Since the total field is the superposition of the two modes, the field pattern at the output port is an exact replica of that existing in the input port. Because the FW-CBCPW is so designed, it shows 50 Ω characteristic impedance when the side planes are grounded. Therefore, the signal generator of 50 Ω internal impedance can transmit power into the FW-CBCPW without reflection. As a result, we observe an almost perfect signal transmission at 16.5 GHz from the theoretic calculation. However, the measured transmission band is shifted by about 1.4 GHz higher than the theoretical one. Our experience in the through line analysis indicates that above 16 GHz, the little difference between theoretical and practical propagation constants of the CPW and MSL modes, say 1.0% deviation, will have the resonant frequency shifted by more than 0.17 GHz and the transmission band shifted by approximately 1.0 GHz. Since the propagation constants of the individual CPW and MSL modes may deviate appreciably from the actual values of the coupled system, particularly in the high frequencies, the good agreement in the low frequency range and the discrepancy at high frequencies between the theory and experiment should be expected.

In summary, the extra MSL mode may result in the undesired resonance or crosstalk in a practical FW-CBCPW circuit. If its presence can not be avoided, we may keep the CBCPW circuit much smaller than a half wavelength
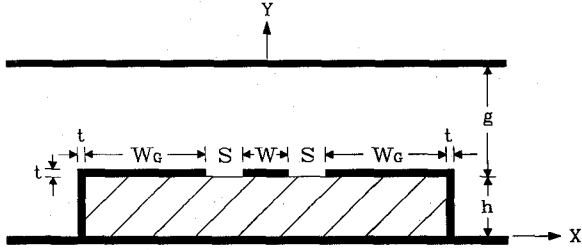
Fig. 8. The cross-sectional geometry of the modified FW-CBCPW with the lateral side-plane edges shorted to the lower ground plane. The structural parameters are given as follows: $W = S = 0.508$ mm, $W_G = 1.0$ mm, $W_D = 0.0$ mm, $h = 0.2$ $g = 0.635$ mm, $t = 17\mu$m, $\sigma = 5.8 \times 10^7$ S/m (copper), and $\epsilon_r = 10.2$.

Fig. 9. The measured transmission ($|S_{21}|$) and reflection ($|S_{11}|$) characteristics of the modified FW-CBCPW through line of Fig. 8. The through line length L is equal to 38.1 mm.

of the MSL mode. The MSL mode can have its wavelength approximated by $\lambda_o/\sqrt{\epsilon_r}$, where ϵ_r is the relative dielectric constant of the CBCPW substrate [31]. Therefore, the terminated FW-CBCPW through line should have its physical dimension satisfying the following condition to avoid resonance or crosstalk:

$$L_{\max} << (\lambda_o/\sqrt{\epsilon_r})/2 \qquad (11)$$

where λ_o is the free-space wavelength.

V. THE IMPROVEMENT ON THE THROUGH LINE PERFORMANCE OF FW-CBCPW

As the problem of the MSL mode in the FW-CBCPW circuit is identified, we may adopt a similar method reported in [17] to suppress the MSL mode by uniformly grounding the two outer edges of the side planes. Fig. 8 shows the cross-sectional geometry of the modified FW-CBCPW structure. The material constants and the structural parameters used in the through line test circuit are also listed in Fig. 8. The electromagnetic field of the dominant CPW mode is confined mostly by the surrounding conductor. Fig. 9 shows the measured magnitude of transmission coefficient ($|S_{21}|$) and reflection coefficient ($|S_{11}|$) from 0.066 GHz to 26.5 GHz. The experimental results demonstrate very smooth through line performance below 17 GHz, above which appreciable amount of transmission losses and resonance occur. To understand why this happens, Fig. 10 shows the dispersion characteristics of the modified FW-CBCPW. Note that the first higher order mode leaks below 19 GHz and has appreciable leakage effect ($\alpha/k_o < 1.0$) from 17 to 19 GHz. By applying (12), we may estimate that the first resonant frequency located at 17.7 GHz.

$$\beta_{\text{Leak}}(f_n) \times L = n\pi. \qquad (12)$$

It is close to the experimental data shown in Fig. 9. The other resonant frequencies can also be estimated similarly. We may conclude that the resonant phenomenon is mainly due to the excitation of the first higher order mode. The modified FW-CBCPW becomes overmoded above 17 GHz and results in similar anomalous resonant phenomenon observed in the preceding section. In practice, the modified FW-CBCPW should be designed with proper dimension so that extra higher order mode will not be excited.
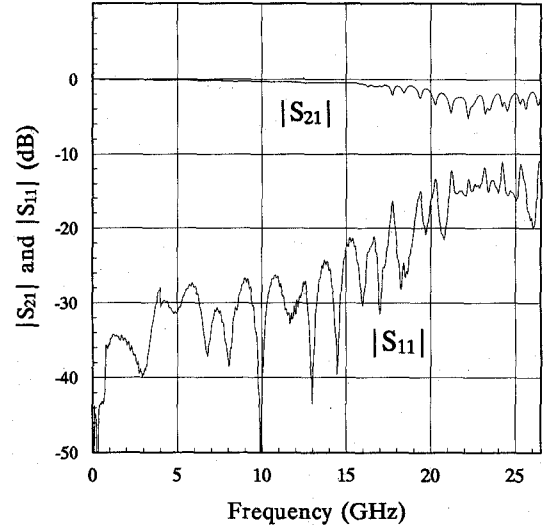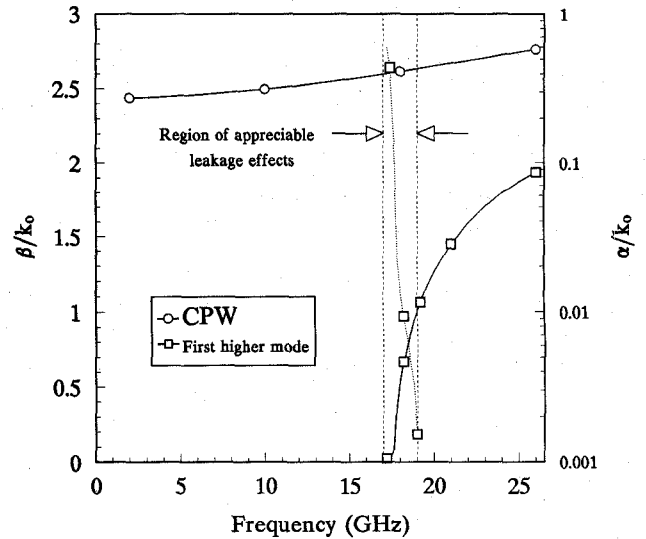

Fig. 10. Dispersion characteristics of the modified FW-CBCPW as shown in Fig. 8. -o- Normalized phase constants of CPW mode; -□- Normalized phase constants of the first higher order mode; ..□.. Normalized leaky constants of the first higher order mode.

VI. CONCLUSION

An FW-CBCPW of finite-width side planes and substrate is treated as a system of three coupled microstrip lines. The dispersion characteristics of the FW-CBCPW are obtained by rigorous full-wave mode-matching method incorporating the metal modes. A general 4-port network representation of the half circuit of the FW-CBCPW through line is derived while the normalizing impedance matrix that defines the boundary condition of the test fixture is obtained. The measured scattering parameters agree very well with the theoretic results. The anomalous resonant phenomenon associated with the scattering parameters of the through line is related to the multiple of half-wavelength resonance of the extra MSL (microstrip-like) mode. Such resonance exists almost periodically between dc and 26.5 GHz in our particular case study. An experimental study on a modified FW-CBCPW through line with two side
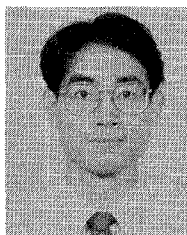
planes grounded on the side wall demonstrates a smooth transmission characteristic below 17 GHz. Above 17 GHz, extra higher order modes may appear and result in a similar resonant phenomenon. When the overmoded situation can not be avoided, the FW-CBCPW length should be kept as short as possible, i.e., much less than the half wavelength of MSL mode, to avoid excessive cross-talk (coupling) or possible resonance. If a mode-suppression technique, such as the one shown in Section V, is applied to the modified FW-CBCPW to eliminate the MSL mode, a first higher order mode will exist and produce the undesired resonant phenomenon in the through-line measurement. In practice, the modified FW-CBCPW should keep its side-plane width small enough such that the onset frequency of the extra higher order mode is well beyond the desired upper frequency limit of the CBCPW circuit.

ACKNOWLEDGMENT

REFERENCES

[1] C. P. Wen, "Coplanar waveguide: A surface strip transmission line suitable for nonreciprocal gyromagnetic device application," *IEEE Trans. Microwave Theory Tech.*, vol. MTT-17, pp. 1087–1090, 1969.

[2] J. K. Hunton, "A microwave integrated circuit balanced mixer with broad-bandwidth," *Proc. (IEEE-MTT) Microelectronics Symp.*, pp. A3.1–A3.2, 1969.

[3] M. Riaziat, I. Zubeck, S. Bandy, and G. Zdasiuk, "Coplanar waveguides used in 2-18 GHz distributed amplifier," in *IEEE MTT-S Int. Microwave Symp. Digest.* pp. 337–338, June 1986.

[4] D. Neuf and S. Spohrer, "Double balanced, coplanar, image rejection mixer uses monolithic MESFET QUAD," in *IEEE MTT-S Int. Microwave Symp. Digest.* pp. 843–846, 1991.

[5] M. Riaziat, E. Par, G. Zdasiuk, S. Bandy and M. Glenn, "Amplifier and frequency doubler monolithic millimeter-wave CPW circuits using 0.25-μm-gate AlGaAs HEMT," in *IEEE MTT-S Int. Microwave Symp. Digest.* pp. 525–528, 1989.

[6] Y. C. Shih and T. Itoh, "Analysis of conductor-backed coplanar waveguide," *Electron. Letters*, vol. 18, pp. 538–540, June 1982.

[7] L. Wiemer and R. H. Jansen, "Reciprocity related definition of strip characteristic impedance for multiconductor hybrid-mode transmission lines," *Microwave and Optical Technology Letters*, vol. 1, no. 1, pp. 22–25, Mar. 1988.

[8] V. Tripathi and H. Lee, "Spectral-domain computation of characteristic impedances and multiport parameters of multiple coupled lines," *IEEE Trans. Microwave Theory Tech.*, vol. MTT-37, pp. 215–220, Jan. 1989.

[9] J.-T. Kuo and C.-K. C. Tzuang, "Termination for minimal reflection of high-speed pulse propagation along multiple coupled microstrip lines," *Proc. SPIE*, vol. 1389, pp. 156–160, 1990.

[10] A. A. Oliner, "Leakage from higher modes on microstrip line with application to antennas," *Radio Sci.*, vol. 22, no. 6, pp. 907–912, Nov. 1987.

[11] C.-K. C. Tzuang, C.-D. Chen, and S. T. Peng, "Full-wave analysis of lossy quasi-planar transmission line incorporating the metal modes," *IEEE Trans. Microwave Theory Tech.*, vol. MTT-38, pp. 1792–1799, Dec. 1990.

[12] C.-D. Chen, C.-K. C. Tzuang, and S. T. Peng, "Skin-effect current distribution of a unilateral finline with finite conductivity," in *IEEE MTT-S Microwave Symp. Digest.* pp. 773–776, June 1991.

[13] C.-D. Chen, C.-K. C. Tzuang, and S. T. Peng, "Full-wave analysis of a lossy rectangular waveguide containing rough inner surfaces," *IEEE Microwave Guided Wave Letts.*, vol. 2, pp. 180–181, May 1992.

[14] C.-C. Tien, C.-K. C. Tzuang, and S. T. Peng, "Effects of metal thickness and finite substrate width on leaky waves in coupled microstrip lines," in *IEEE MTT-S Microwave Symp. Digest.* pp. 499–502, June 1992.

[15] User Manual of CASCADE MICROTECH Summit 10000 Semi-Automatic Probe Station.

[16] Tektronix 1991 Catalog, pp. 52–53.

[17] Y.-C. Shih, "Broadband characterization of conductor-backed coplanar waveguide using accurate on-wafer measurement techniques," *Microwave J.*, Apr. 1991, pp. 95–105.

[18] J. B. Knorr and K. D. Kuchler, "Analysis of coupled slots and coplanar strips on dielectric substrate," *IEEE Trans. Microwave Theory Tech.*, vol. MTT-23, pp. 541–548, 1975.

[19] T. Itoh, "Spectral domain immittance approach for dispersion characteristics of generalized printed transmission lines," *IEEE Trans. Microwave Theory Tech.*, vol. MTT-28, pp. 733–736, July 1980.

[20] T. Kitazawa, Y. Hayashi, and M. Suzuki, "A coplanar waveguide with thick metal-coating," *IEEE Trans. Microwave Theory Tech.*, vol. MTT-24, pp. 604–608, Sept. 1976.

[21] R. Sorrentino, G. Leuzzi, and A. Silbermann, "Characteristics of metal-insulator semiconductor coplanar waveguides for monolithic microwave circuits," *IEEE Trans. Microwave Theory Tech.*, vol. MTT-32, pp. 410–416, Apr. 1984.

[22] Y. Fukuoka, Y.-C. Shih, and T. Itoh, "Analysis of slow-wave coplanar waveguide for monolithic integrated circuits," *IEEE Trans. Microwave Theory Tech.*, vol. MTT-31, pp. 567–573, July 1983.

[23] C.-K. C. Tzuang and T. Itoh, "Finite element analysis of a slow-wave Schottky contact printed line," *IEEE Trans. Microwave Theory Tech.*, vol. MTT-34, pp. 1483–1489, Dec. 1986.

[24] C.-K. C. Tzuang and T. Itoh, "High-speed pulse transmission along a slow-wave CPW for monolithic microwave integrated circuits," *IEEE Trans. Microwave Theory Tech.*, vol. MTT-35, pp. 697–704, Aug. 1987.

[25] T. H. Wang and T. Itoh, "Compact grating structure for application to filter and resonators in monolithic microwave integrated circuits," *IEEE Trans. Microwave Theory Tech.*, vol. MTT-35, pp. 1176–1182, Dec. 1987.

[26] R. H. Jansen, "Hybrid mode analysis of end effects of planar microwave and millimeter wave transmission lines," *Proc IEE.*, vol. 128, pt. H, Apr. 1981, pp. 77–86.

[27] R. W. Jackson, "Considerations in the use of coplanar waveguide for millimeter-wave integrated circuits," *IEEE Trans. Microwave Theory Tech.*, vol. MTT-34, pp. 1450–1456, Dec. 1986.

[28] H. Shigesawa, M. Tsuji, and A. A. Oliner. "Conductor-backed slot line and coplanar waveguide: Dangers and full-wave analyses," in *IEEE MTT-S Int. Microwave Symp. Digest*, pp. 199–202, 1988.

[29] _____, "A new mode-coupling effect on coplanar waveguides of finite width," in *IEEE MTT-S Int. Microwave Symp. Digest*, pp. 1063–1066, 1990.

[30] M. Tsuji, H. Shigesawa, and A. A. Oliner, "New interesting leakage behavior on coplanar waveguides of finite and infinite widths," *IEEE Trans. Microwave Theory Tech.*, vol. MTT-39, pp. 2130–2136, Dec. 1991.

[31] R. W. Jackson, "Mode conversion at discontinuities in finite-width conductor-backed coplanar waveguide," *IEEE Trans. Microwave Theory Tech.*, vol. MTT-37, pp. 1582–1589, Oct. 1989.

[32] M. Tsuji and H. Shigesawa, "The feature of the narrow-pulse transmission on conventional coplanar waveguides when power leakage is present," in *IEEE MTT-S Microwave Symp. Digest*, pp. 991–994, June 1992.

[33] M. Riaziat, I. J. Feng, R. Majidi-Ahy, and B. A. Auld, "Single-mode operation of coplanar waveguides," *Electron. Letts.*, vol. 23, no. 24, pp. 1281–1283, Nov. 1987.

[34] M. A. Magerko, L. Fan, and K. Chang, "Multiple dielectric structures to eliminate moding problems in conductor-backed coplanar waveguide MIC's *IEEE Microwave and Guided Letts.*, vol. 2, pp. 257–259, June 1992..

[35] C.-K. C. Tzuang and J.-D. Tseng, "A full-wave mixed potential mode-matching method for the analysis of planar or quasi-planar transmission lines," *IEEE Trans. Microwave Theory Tech.*, vol. MTT-39, pp. 1701–1711, Oct. 1991.

[36] K. C. Gupta, R. Garg, and R. Chadha, *Computer-Aided Design of Microwave Circuits.* New York: Artech, 1981.
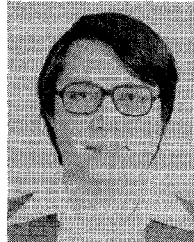
Ching-Cheng Tien was born in Taiwan on March 19, 1966. He received the B.S. degree in communication engineering from the National Chiao Tung University, Hsinchu, Taiwan, in 1988 and the Ph.D. degree at the same university, in 1993. His current research interests include the analysis and design of microwave and millimeter-wave components.

Ching-Kuang C. Tzuang (S'84–M'86–SM'92) was born in Taiwan on May 10, 1955. He received the B.S. degree in electronic engineering from the National Chiao Tung University, Hsinchu, Taiwan, in 1977 and the M.S. degree from the University of California at Los Angeles, CA, in 1980. From February 1981 to June 1984, he was with TRW, Redondo Beach, CA, working on analog and digital monolithic microwave integrated circuits. He received the Ph.D. degree in electrical engineering in 1986 from the University of Texas, Austin, TX, where he worked on high-speed transient analysis of monolithic microwave integrated circuits. Since September 1986, he has been with the Institute of Communication Engineering, National Chiao Tung University, Hsinchu, Taiwan, Republic of China. His research activities involve the design and development of millimeter-wave and microwave active and passive circuits and the field theory analysis and design of various quasi-planar integrated circuits.

Chung-Chi Chang was born in Shanghai, China, in 1946. He received the B.S. and M.S. degrees in electrical engineering from Chun Cheng Institute of Technology, Taoyun, Taiwan, in 1970 and 1975, respectively. In 1982 he received the Ph.D. degree in Southern Methodist University, Dallas, Texas.

Dr, Chang has over 12 years of microwave device and circuit experiences. From 1975 to 1979, he was Assistant Researcher at the electronic system division, Chung Shan Institute of Science and Technology (CSIST), Taiwan. There he was responsible for design, fabrication and testing of hybrid microwave integrated circuits. Successfully completed circuits were parallel coupled BPF, coupler, mixer, Gunn-diode oscillator. After he got his Ph.D. degree in 1982, he went back to CSIST and worked as an associate researcher to manufacture both thin film and thick film hybrid integrated circuits. Since 1986, Dr. Chang has been in charge of the Solid State Device Section in CSIST. A lot of different kinds of semiconductor devices, components, circuit modules, and technologies have been developed such as high power PIN diode, HEMT, photonic device, microwave circuit module, frequency synthesizer, and SMT, etc. As a matter of fact, most of these products have really been used in the systems. Dr. Chang has also worked as a part-time associate professor in National Chiao Tung University, Hsinchu, Taiwan, since 1989.

S. T. Peng (M'74–SM'82–F'88) was born in Taiwan, Republic of China, on February 19, 1937. He received the B.S. degree in electrical engineering from the National Cheng Kung University in 1959, the M.S. degree in electronics from the National Chiao Tung University in 1961, both in Taiwan, and the Ph.D. degree in electrophysics from the Polytechnic Institute of Brooklyn, Brooklyn, NY, in 1968.

After 1968, he held various research positions with the Polytechnic Institute of Brooklyn. From 1983 to 1990, he was a Professor of Electrical Engineering and Director of the Electromagnetics Laboratory at the New York Institute of Technology, Old Westbury, NY. Since 1991, he has been a Professor of Communication Engineering at the National Chiao Tung University, Taiwan. He has been active in the field of wave propagation, radiation, diffraction, and nonlinear electromagnetics and has published numerous papers on electromagnetics, optics, and acoustics. Dr. Peng is a member of Sigma Xi.